

SEA WAVE PATTERN EVALUATION

Part 4 Report: Extension to Multihulls and Finite Depth

E.O. Tuck, D.C. Scullen and L. Lazauskas

Applied Mathematics Department
The University of Adelaide

19 June 2000

Abstract

This is the fourth report in a series describing a computer program *SWPE* which is intended eventually to provide a full description of the wave elevation and flow field created by a surface-piercing or submerged body moving steadily forward in still water of constant depth. The first two reports [5, 6] (produced as a result of a 1998-9 contract with The University of Adelaide) provided results in the far field. The third report [7], dated 31st January 2000 from Scullen & Tuck Pty Ltd, included near-field effects. The present report discusses extensions to multihulls and finite depth.

The front cover of this report is a contour plot of wave elevations predicted by *SWPE* for a catamaran consisting of two Wigley hulls, each of length 100m, travelling side-by-side at a speed of 30 knots, equivalent to a Froude number of 0.53, separated by a distance equal to half their length.

1 Introduction

In the present report, we expand upon the work of the previous three reports, to extend the ability of SWPE to cater for multiple hulls and also to determine the far-field wave pattern for vessels sailing in a sea of finite depth.

It is a straight-forward exercise to extend SWPE to cater for fleets of ships or multihulls. Since SWPE assumes a linearised free-surface, we can sum the wave elevations or fluid velocities due to each hull individually, to yield the total effect due to their combination. This is implemented by an outer iteration over each hull, before reporting the wave elevations and fluid velocities. As a result, SWPE is now capable of determining the total field for multihulls — not just the far-field as was specified in the Statement of Requirements for the present contract.

The other, more difficult, enhancement to SWPE is that it can now be used to determine the far-field wave pattern produced by vessels travelling in water of finite depth. This is done by generalising the free-wave spectrum concept to water of uniform depth h . As specified in the contract, the present program allows this generalisation only in the far field. Determining the near field in finite depth would require numerical evaluation of a quadruple integral of an even more complicated nature than that for infinite depth, and no optimised and economised procedures are available at this time for these integrals. Such economisations were an essential feature of the infinite-depth near-field previous version SWPE3.0 of SWPE. Although direct numerical integration is available for the finite-depth near field, the resulting code would be computationally expensive, and any generalisation to this case would require careful study.

It is therefore now possible within SWPE to determine the total field for multiple hulls, with or without transom sterns, sailing in a deep sea. In addition, it is possible to determine the far field for these same craft, when in water of finite depth. Again, the ability to implement multihulls in finite depth has been provided in excess of the formal requirements of the present contract.

Section 2 of this report details the manner in which the flow about multiple hulls is determined, and shows examples of the surface elevations predicted by SWPE4.0 for certain combinations of hulls. Section 3 gives the theory for determining the far-field flow for vessels travelling in water of finite depth, and Section 4 shows examples of how the wave pattern varies as the speed of the vessel increases toward and through the critical speed \sqrt{gh} .

2 Multihull theory and examples

As stated in the introduction, it is a simple matter to enhance SWPE so that it can determine the wave pattern produced by a combination of ships. The simplicity is entirely dependent upon the fact that SWPE implements a *linearised* free-surface boundary condition. As such, the sum of flows produced by any two (or more) hulls will satisfy the free-surface condition. Thus, the flow due to a combination of ships is, under the assumption of a linearised free-surface, simply the combination of the flows that would be produced by the ships as individuals.

We are therefore able to implement this as an outer loop in SWPE, determining the wave pattern for each hull in turn, and summing the results. The user need only supply SWPE with the offsets for each additional hull and its location. Note that the complete range of SWPE's options (near-field evaluation, effect of viscosity, influence of the transom-stern condition, and finite-depth effects) is now available for combinations of hulls.

Figure 1 demonstrates the wave pattern due to two identical Wigley hulls, each of length 100m, travelling side by side with a separation equal to half their length, and at a speed of 30 knots. This arrangement is of course analogous to a conventional catamaran. In all figures presented in this report, we have used an eddy viscosity of $0.005\text{m}^2\text{s}^{-1}$ when computing the wave pattern. The computations have been performed on a grid of 301×301 points.

Figure 2 shows the combined wave pattern of two identical DDG51 destroyers (DTMB Model 5415), each of length 142m, travelling in tandem at a speed of 30 knots and separated by a length of approximately 87m, as though one vessel were being towed by the other.

As a demonstration of the versatility of SWPE, Figure 3 shows the wave pattern produced by three different vessels — a DDG51 destroyer, a US Los Angeles class submarine and a Wigley-hulled catamaran, each travelling at 30 knots. The submarine's depth is such that it is only just submerged.

3 Finite-depth thin-ship theory

3.1 Introduction

Michell [3] formulated his thin-ship theory in water of finite depth, but only derived the potential and wave resistance for infinite depth. Havelock [1] presented formulae for free wave patterns and wave resistance in finite depth. Lunde [2] pro-

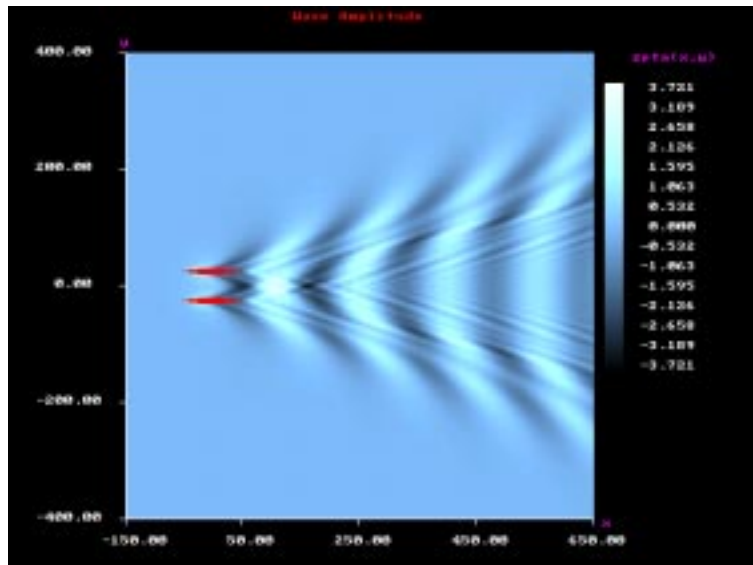


Figure 1: Wave pattern due to a catamaran comprised of two identical Wigley hulls, each of length 100m, with a separation equal to half their length, travelling at a speed of 30 knots.

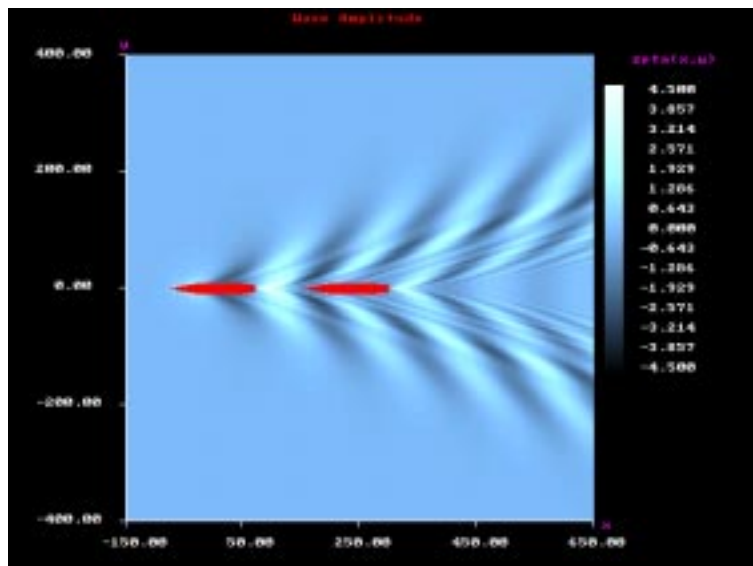


Figure 2: The combined wave pattern of two identical DDG51 destroyers each of length 142m, travelling in tandem at a speed of 30 knots and separated by approximately 87m.

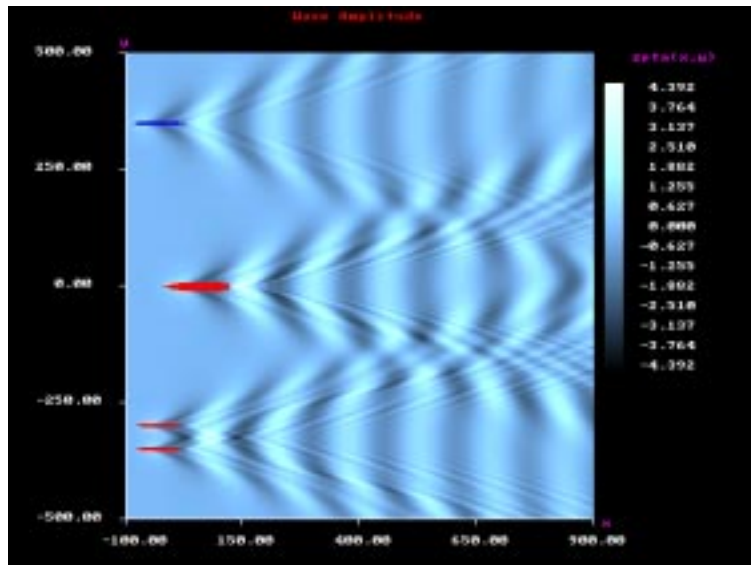


Figure 3: Combined wave pattern produced by a DDG51 destroyer, a US Los Angeles class submarine and a Wigley-hulled catamaran, each travelling at 30 knots. The submarine (uppermost vessel) is only just submerged.

vided various derivations of finite-depth wave resistance formulas, including one for a thin ship in the sense of Michell, but no wave patterns. For convenience, we re-derive here the full finite-depth theory, and in particular the free-wave pattern far behind the ship.

3.2 The Michell boundary-value problem

We have to solve Laplace's equation

$$\phi_{xx} + \phi_{yy} + \phi_{zz} = 0 \quad (1)$$

in $-h < z < 0$, with bottom condition

$$\phi_z = 0 \quad \text{on} \quad z = -h, \quad (2)$$

and the Kelvin free-surface condition

$$k_0 \phi_z + \phi_{xx} = 0 \quad \text{on} \quad z = 0, \quad (3)$$

where $k_0 = g/U^2$. The ship is supposed laterally (y -wise) symmetric, with offsets $y = \pm Y(x, z)$, and the linearised (Michell) hull boundary condition is

$$\phi_y = \pm U Y_x(x, z) \quad \text{on} \quad y = 0_{\pm}. \quad (4)$$

3.3 Fourier transformation

Define the double Fourier transform

$$\Phi(x, y, z) = \frac{1}{\pi^2} \int_{-\infty}^{\infty} dx e^{i\lambda x} \int_0^{\infty} dy \cos \mu y \phi(x, y, z) \quad (5)$$

with inverse

$$\phi(x, y, z) = \int_{-\infty}^{\infty} d\lambda e^{-i\lambda x} \int_0^{\infty} d\mu \cos \mu y \Phi(z; \lambda, \mu). \quad (6)$$

Then the Laplace equation (1) subject to the Michell condition (4) yields an inhomogeneous ordinary differential equation for Φ , namely

$$\frac{d^2 \Phi}{dz^2} - k^2 \Phi = \frac{2U}{\pi} \overline{Y}_x(z; \lambda) \quad (7)$$

where \overline{Y}_x is the x -Fourier transform of the hull slope Y_x , i.e.

$$\overline{Y}_x(z; \lambda) = \frac{1}{2\pi} \int_{-\infty}^{\infty} dx e^{i\lambda x} Y_x(x, z) \quad (8)$$

and $k^2 = \lambda^2 + \mu^2$.

3.4 Solution for the Fourier transform

The most general solution of (7) subject to (2) is

$$\Phi = \frac{2U}{\pi k} \int_{-h}^z \overline{Y}_x(\zeta; \lambda) \sinh k(z - \zeta) d\zeta + C \cosh k(z + h) \quad (9)$$

for some constant C , and the choice of C such that (3) holds is

$$C = -\frac{2U}{\pi k} \int_{-h}^0 \overline{Y}_x(\zeta; \lambda) \frac{k_0 k \cosh k\zeta + \lambda^2 \sinh k\zeta}{k_0 k \sinh kh - \lambda^2 \cosh kh} d\zeta. \quad (10)$$

It is now only necessary to invoke the inverse transform (6) to complete the solution for ϕ . In general there is a simple pole where the denominator of (10) vanishes, and it is necessary in doing the inverse Fourier integrals to avoid this pole carefully in such a way that the radiation condition is satisfied, i.e. that there are no waves upstream at $x = -\infty$.

3.5 Free-surface elevation

We are particularly interested in the free-surface elevation $z = Z(x, y)$ where $Z = -(U/g)\phi_x(x, y, 0)$. This has double Fourier transform $\bar{Z}(\lambda, \mu)$ where

$$\bar{Z} = -\frac{i\lambda/\pi^2}{k_0 k \sinh kh - \lambda^2 \cosh kh} \iint Y_x(\xi, \zeta) e^{-i\lambda\xi} \cosh k(\zeta + h) d\xi d\zeta. \quad (11)$$

Inverse Fourier transformation yields

$$Z(x, y) = \int_{-\infty}^{\infty} d\lambda e^{-i\lambda x} \int_0^{\infty} d\mu \cos \mu y \bar{Z}(\lambda, \mu) \quad (12)$$

If we make the polar conversion $\lambda = k \cos \theta, \mu = k \sin \theta$ in wave-number space, we find

$$Z(x, y) = 2\Re \int_0^{\pi/2} d\theta \int_0^{\infty} dk k e^{-ikx \cos \theta} \cos(ky \sin \theta) \bar{Z}(k \cos \theta, k \sin \theta) \quad (13)$$

and it is then apparent that the radiation condition is satisfied if the path of k -integration is diverted above the pole, which occurs where $k_0 k \sinh kh - \lambda^2 \cosh kh = 0$, or

$$k = k_0 \sec^2 \theta \tanh kh. \quad (14)$$

To extend SWPE to include finite depth in the near field, it would be necessary to evaluate (13) subject to (11), which is a formidable (quadruple integration) task and was not proposed in the current contract. Instead, we confine attention to the triple integral which describes the far field, as follows.

3.6 Far-field approximation

The free waves at $x = +\infty$ are obtained from the residue at the pole. Specifically, if we change to a path of integration going under the pole, the new k -integral will tend to zero as $x \rightarrow +\infty$ instead of $x \rightarrow -\infty$. The difference between these two integrals is $-2\pi i$ times the residue at the pole, and this must be the far field wave. Thus as $x \rightarrow +\infty$, we have $Z \rightarrow Z^0$, where

$$Z^0(x, y) = \Re \int_{-\pi/2}^{\pi/2} A(\theta) e^{-ik(x \cos \theta + y \sin \theta)} d\theta. \quad (15)$$

After some manipulation, we find the Michell formula for the free-wave spectrum $A(\theta)$ in terms of the hull slope $Y_x(x, y)$ to be

$$A(\theta) = \frac{2}{\pi} \sec \theta \frac{k}{1 - k_0 h \sec^2 \theta \operatorname{sech}^2 kh} \iint Y_x(x, z) \frac{\cosh k(z + h)}{\cosh kh} e^{ikx \cos \theta} dx dz. \quad (16)$$

This expression can be integrated by parts to give

$$A(\theta) = -\frac{2i}{\pi} \frac{k^2}{1 - k_0 h \sec^2 \theta \operatorname{sech}^2 kh} \left[\iint Y(x, z) \frac{\cosh k(z+h)}{\cosh kh} e^{ikx \cos \theta} dx dz - \frac{1}{ik \cos \theta} e^{ikx_s \cos \theta} \int Y(x_s, z) \frac{\cosh k(z+h)}{\cosh kh} dz \right], \quad (17)$$

where $x = x_s$ at the stern. Note that the second term inside the square brackets of (17) vanishes if there is no transom.

The above holds for all θ in the subcritical range $k_0 h > 1$. In the supercritical range $k_0 h < 1$, the spectrum A is identically zero for all $|\theta| < \theta_0$ where $\cos \theta_0 = k_0 h$.

The formal large- h limit of the above formulae for the spectrum follows immediately, since $k \rightarrow k_0 \sec^2 \theta$. The denominator expression $1 - k_0 h \sec^2 \theta \operatorname{sech}^2 kh$ approaches 1, and the ratio $\cosh k(z+h)/\cosh kh$ approaches $\exp(-kz)$. Thus we recover the infinite-depth result, c.f. Tuck and Lazauskas [4]

$$A(\theta) = -\frac{2i}{\pi} k^2 \iint Y(x, z) e^{-kz} e^{ikx \cos \theta} dx dz \quad (18)$$

as programmed in earlier versions of SWPE.

Replacement of (18) by (17) to allow finite depth h is straightforward in principle, but requires care in implementation, and it is this that has been provided in SWPE4.0.

4 Finite-depth examples

In this section we show the effect of sea depth on the surface elevations as predicted by SWPE for a DDG51 destroyer. In the figures which are to follow, the vessel has length 142m and is travelling at a speed of 30 knots, so the length-based Froude number ($F_L = U/\sqrt{gL}$) is 0.4136. As with the multihull examples, an eddy viscosity of $0.005\text{m}^2\text{s}^{-1}$ has been introduced.

Figure 4 shows the elevations when the sea is of infinite depth. The wake is contained within the classical wedge with angle 39° , and the purely-transverse waves have a wavelength of $2\pi U^2/g$ or $2\pi L F_L^2$, which corresponds here to 154 metres.

Figure 5 shows the elevations when the sea is of finite depth, with a depth-based Froude number ($F_h = U/\sqrt{gh}$) of 0.8. Depth can be determined from $h = L(F_L/F_h)^2$, and corresponds here to approximately 38 metres. At this depth,

the enveloping wedge has widened slightly, and the transverse wavelength has increased slightly also.

Figure 6 shows a case where the depth-based Froude number is nearing the critical value of one. In this case, the depth-based Froude number is 0.95, corresponding to a depth of approximately 27 metres. The enveloping wedge has widened significantly, and the transverse wavelength has doubled.

Figure 7 shows a supercritical case, with a depth-based Froude number of 1.05, which corresponds to approximately 22 metres depth. The enveloping wedge angle remains widened significantly, but there are no longer any transverse waves, their wavelength having approached infinity.

Figure 8 is for a thoroughly supercritical speed, with a depth-based Froude number of 1.4, corresponding to a depth of approximately 12 metres. The enveloping wedge has narrowed further, and again there are no transverse waves.

As the depth-based Froude number is increased further, the angle of the enveloping wedge continues to decrease, and the wave pattern contains only diverging waves.

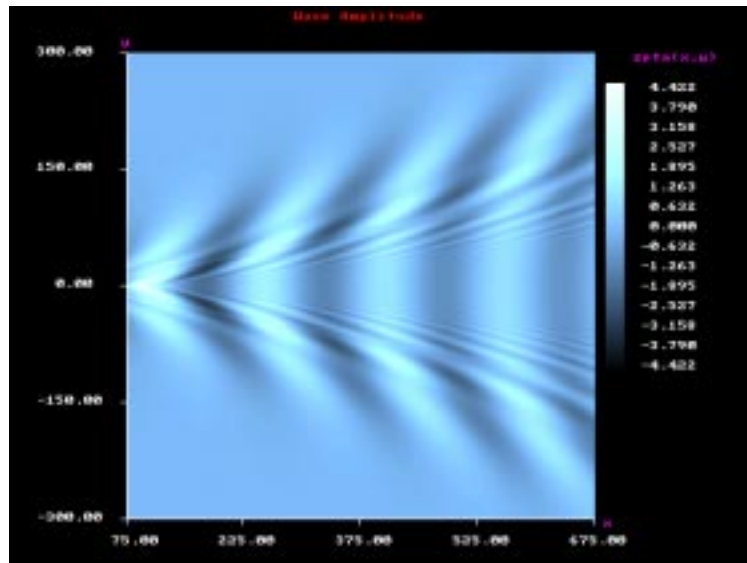


Figure 4: Wake as determined by SWPE for a DDG51 destroyer in deep water and travelling at 30 knots. This corresponds to a length-based Froude number of 0.4136.

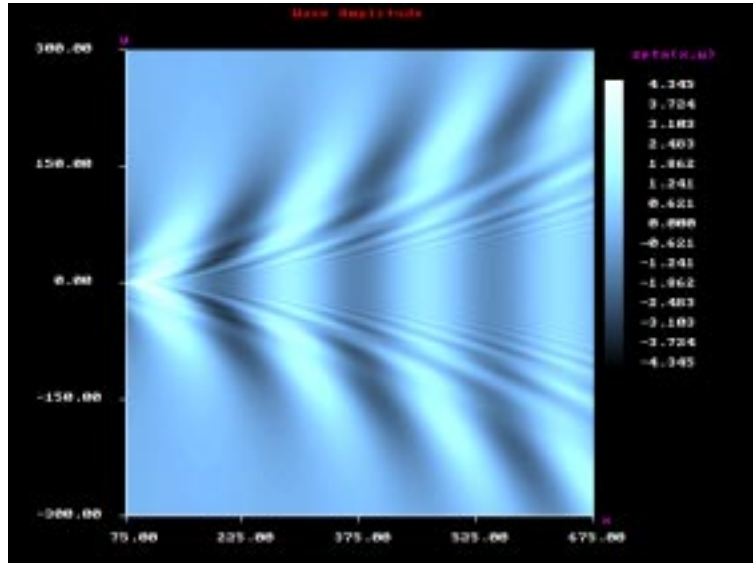


Figure 5: As above, but in water of finite depth, with a depth-based Froude number 0.8, corresponding to water of depth 38m. The enveloping wedge has widened slightly, and the transverse wavelength has increased slightly also.

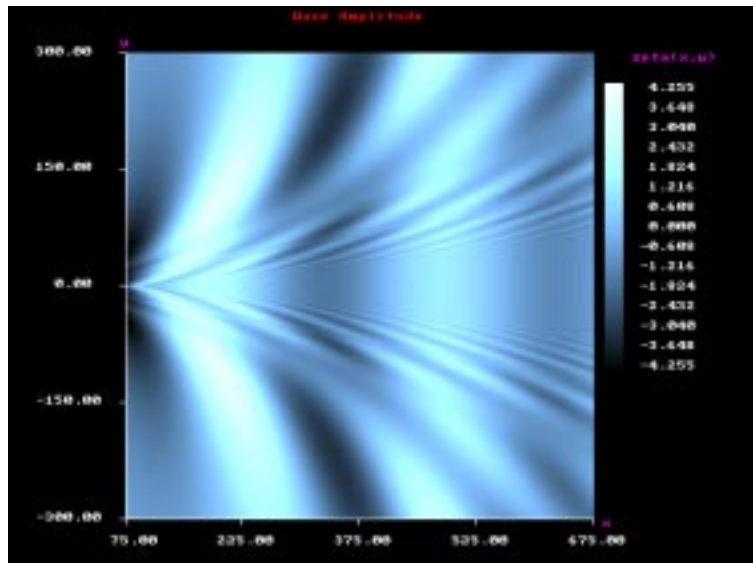


Figure 6: As above, but with a depth-based Froude number 0.95, which corresponds to a water depth of approximately 27m. The enveloping wedge has widened significantly, and the transverse wavelength has doubled.

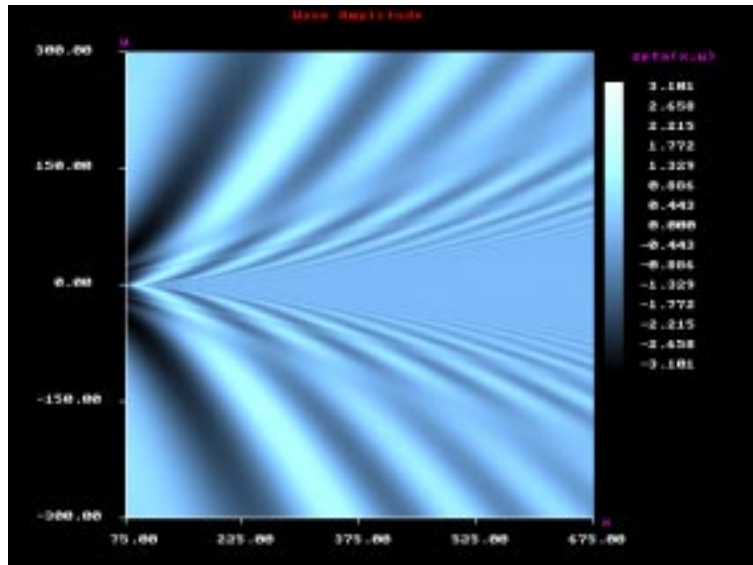


Figure 7: As above, but with a depth-based Froude number 1.05, or depth 22m. Note the complete absence of transverse waves and large Kelvin angle in this just-supercritical flow.

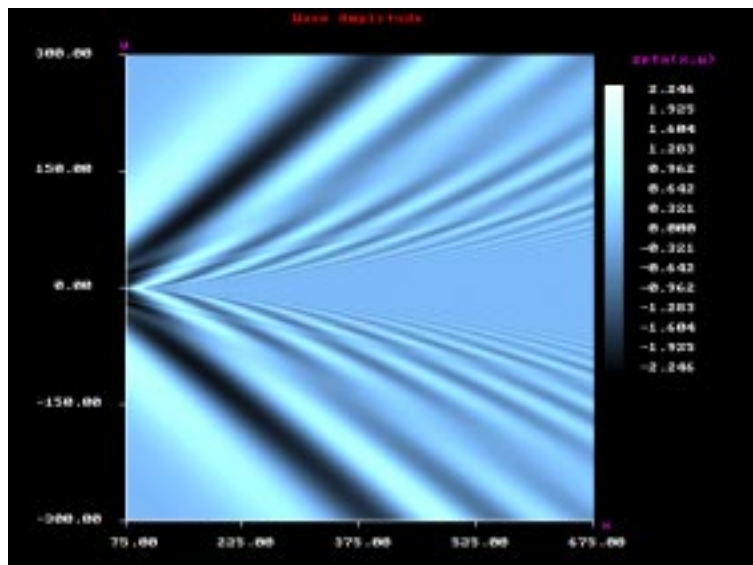


Figure 8: As above, but with a depth-based Froude number 1.4, which corresponds here to a depth of approximately 12m. The enveloping wedge is narrowing, and there are no transverse waves.

References

- [1] Havelock, T.H. *The calculation of wave resistance*, Proc. Roy. Soc. Lond. Ser. A, **144** 514–521 (1934).
- [2] Lunde, J.K. *On the linearized theory of wave resistance for displacement ships in steady and accelerated motion*, Trans SNAME **59** 25–85 (1951).
- [3] Michell, J.H. *The wave resistance of a ship*, Phil. Mag. (5), **45** 106–123 (1898).
- [4] Tuck, E.O. and Lazauskas, L. *Optimum hull spacing of a family of multihulls*, Schiffstechnik **45** 180–195 (1998).
- [5] Tuck, E.O., Lazauskas, L. and Scullen, D.C. *Sea Wave Pattern Evaluation, Part 1 report: Primary code and test results (surface vessels)*, Department of Applied Mathematics, The University of Adelaide (1999).
- [6] Tuck, E.O., Scullen, D.C. and Lazauskas, L. *Sea Wave Pattern Evaluation, Part 2 report: Investigation of accuracy*, Department of Applied Mathematics, The University of Adelaide (1999).
- [7] Tuck, E.O., Scullen, D.C. and Lazauskas, L. *Sea Wave Pattern Evaluation, Part 3 report: Near-Field Waves*, Scullen & Tuck Pty Ltd (2000).